Lawrence Berkeley National Laboratory
Lawrence Berkeley National Laboratory

Title
ANNEALING BEHAVIOR OF HIGH PERMEABILITY AMORPHOUS ALLOYS

Permalink
https://escholarship.org/uc/item/2v4776vw

Author
Rabenberg, L.

Publication Date
1980-06-01

Peer reviewed

eScholarship.org Powered by the California Digital Library
University of California

MASTER

LBL-10995

Lawrence Berkeley Laboratory
UNIVERSITY OF CALIFORNIA

Materials & Molecular
Research Division

ANNEALING BEHAVIOR OF HIGH PERMEABILITY AMORPHOUS ALLOYS

Llewellyn Rabenberg
(M.S. thesis)

June 1980

RECEIVED BY TIC SEP 2 1980

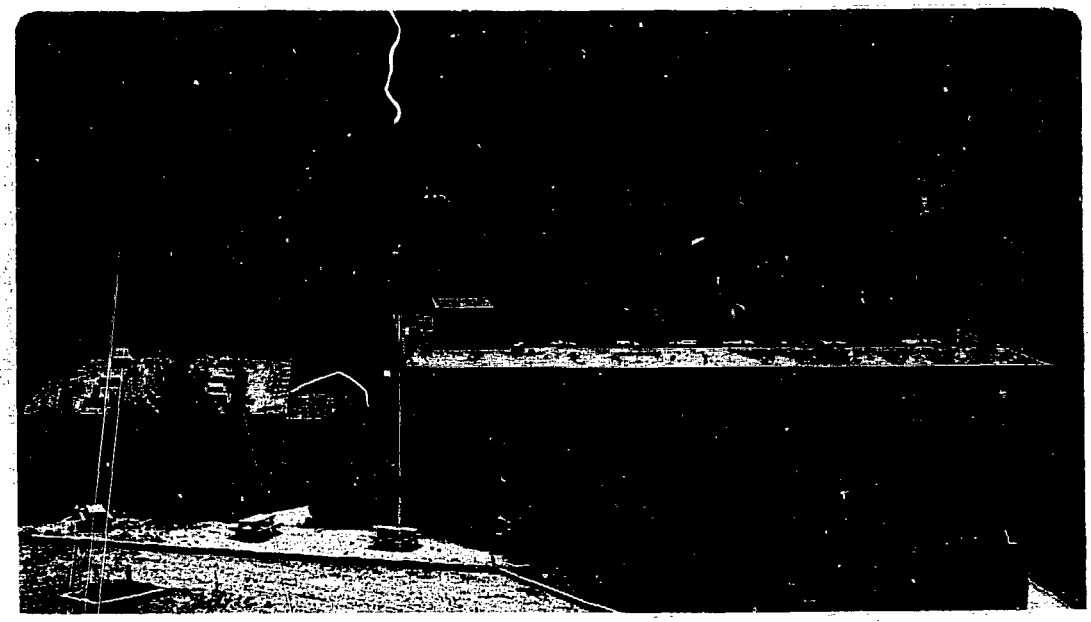

Prepared for the U.S. Department of Energy under Contract W-7405-ENG-48

M.S. Thesis

ANNEALING BEHAVIOR OF HIGH PERMEABILITY AMORPHOUS ALLOYS

Llewellyn Rabenberg

Department of Materials Science and Mineral Engineering

Lawrence Berkeley Laboratory

University of California

Berkeley, California 94720

June 1980

DISCLAIMER

[redacted]

DISTRIBUTION OF THIS DOCUMENT IS UNLIMITED

This work supported by the U.S. Department of Energy, Office of Basic Sciences, under Contract No. W-7405-ENG-48.

TABLE OF CONTENTS

ABSTRACT

The effects of low temperature annealing on the magnetic properties of the amorphous alloy $Co_{71.4}Fe_{4.6}Si_{9.6}B_{14.4}$ have been investigated. Annealing this alloy below 400°C results in magnetic hardening; annealing above 400°C but below the crystallization temperature results in magnetic softening. Above the crystallization temperature the alloy hardens drastically and irreversibly.

Conventional and high resolution transmission electron microscopy have been used to show that the magnetic property changes at low temperatures occur while the alloy is truly amorphous. By imaging the magnetic microstructures, Lorentz electron microscopy has been able to detect the presence of microscopic inhomogeneities in this alloy.

The low temperature annealing behavior of this alloy has been explained in terms of atomic pair ordering in the presence of the internal molecular field. Lorentz electron microscopy has been used to confirm this explanation.

ACKNOWLEDGEMENTS

The author wishes to thank Professor Gareth Thomas for continued guidance and support, Dr. R. K. Mishra for helpful insight, analysis and encouragement, and Professors D. Hess and M. Merriam for their appraisals of the manuscript.

Special thanks go to O. Kohmoto and T. Ojima at TDK Electronics Company, R & D Laboratory, for providing the amorphous alloy and the magnetic measurements. The HREM images were prepared by JEOL corporation and the special magnetic stage was provided by G.T. McKinley of Xerox Palo Alto Research Laboratory.

Financial support has been provided through a grant from the National Science Foundation and a California Regents Fellowship from the University of California. Technical staff and facilities were available through the Department of Energy, Lawrence Berkeley Laboratory, Materials and Molecular Research Division.

I. INTRODUCTION

The soft magnetic behavior of most amorphous alloys is readily attributed to their lack of long-range crystal structure.[1] Amorphous alloys, also called metallic glasses, are produced by rapid quenching from the liquid state; quench rates of $10^5 \rightarrow 10^7$ ^{o}C per second are sufficient to cause solidification while preventing crystallization.[1] The soft magnetic properties, high permeability and low coercive force, are indications of the relative ease with which magnetization rotates under the presence of an applied field. The absence of magneto-crystalline anisotropy and crystal defects such as grain boundaries and dislocations allows metallic glasses to present very little resistance to magnetization rotation. Thus, the ideal soft (high permeability/low coercive force) magnet appears to be the isotropic, homogeneous state of the totally amorphous alloy.

In practice, real amorphous alloys often fail to meet the ideal of an isotropic homogeneous mass of ferromagnetic atoms.[1] That a metallic glass is able to accommodate significant departures from the purely random state has been suggested by many experiments, including magnetic field annealing[2,3], small angle x-ray scattering[4], and stress relaxation.[5] These studies suggest that practical metallic glasses are not homogeneous and isotropic. Despite the large number of investigations into amorphous alloy structure[6-9], and annealing behavior[10-14], the characterization and control of anisotropy and heterogeneity in metallic glasses remain matters of scientific and technological interest.

The first splat-quenched amorphous metals (PdSi)[15] and ferromagnetic alloys (FePC)[16] were prepared in 1965 and 1966 by Duwez and his co-workers. The preparation of amorphous FePC alloys was a direct

confirmation of Gubanov's theoretical prediction[17] that an amorphous material could be ferromagnetic. Amorphous alloys remained a laboratory curiosity until Pond and Maddin[18] and Chen and Miller[19] developed techniques for producing continuous ribbons of glassy alloys in 1969 and 1970. The rapid expansion of the field in the 1970s, in terms of the varieties of alloys and associated data is evidenced by the number of review papers which have been published on various aspects of metallic glasses.[1, 20-25]

The metallic glasses which have received the most attention in the literature are the ferromagnetic alloys of transition metals with metalloids (B,C,Si,P). Many of these alloys have complex compositions because an increase in the number of components usually results in a decrease in the difficulty of fabrication.[1] In all cases, the total concentration of metalloids is approximately 20 atomic percent.[26,27] These transition metal-metalloid (TM-M) alloys can be divided into two areas in terms of their magnetic properties and potential applications.[20] The iron-based alloys developed by Allied Chemical Corporation have optimized saturation induction and thermal stability for power transformer applications.[28-35] Alloys designed for magnetic recording are cobalt-based high permeability, zero magnetostriction alloys.[13,14,36]

The use of high saturation induction amorphous alloys in power transformers results in significant reduction in eddy current core losses because of the high electrical resistivity of these alloys.[25] However, the necessary presence of 20 atomic percent metalloid effectively dilutes the magnetization of the amorphous alloys. The amorphous alloy $Fe_{86}B_8C_6$ has the highest known saturation induction[35] at

17.5 kG, but it falls short of that for conventional crystalline 3.2% silicon-iron alloys (20 kG). Crystalline Fe-3.2 Si alloys are still favored in practice, but amorphous alloys may soon become competitive, especially for high frequency applications where the electrical resistivity is more important.

In the absence of magnetocrystalline anisotropy and domain wall pinning sites, magnetoelastic effects (i.e. magnetostriction) may ultimately determine the limit on permeability. Thus, to a first approximation, high ac permeability is designed into metallic glasses by eliminating magnetostriction. This has been the approach taken in order to obtain high ac permeabilities for magnetic recording equipment applications. Empirically it has been found that iron-based alloys are positive magnetostrictive while cobalt based alloys exhibit negative magnetostriction.[1] A ratio of Fe to Co concentrations of approximately 0.06 causes the magnetostriction to average to zero. Alloys with this composition have permeabilities which are similar to those of the supermalloys.[20]

The structure of amorphous alloys has been extensively investigated and several reviews are available.[6-8] The largest part of this work has relied on conventional x-ray diffraction experiments,[37-39] but small angle x-ray diffraction,[4,40] energy dispersive x-ray diffraction,[41] magnetic hyperfine fields,[42] and transmission electron microscopy[9,43-45] all have been tried. These experiments all agree that it is possible to fabricate metallic alloys which are, in fact, non-crystalline.

Metallic glasses are essentially non-equilibrium structures and exhibit a strong driving force for recrystallization. At sufficiently

high temperatures, amorphous alloys decompose into one or more crystalline phases. The large metalloid content (approximately 20 atomic percent) prevents simple transformation into a single crystalline phase. Instead, continuous heating produces a series of metastable phases before final equilibrium phases appear. Crystallization studies using calorimetry,[46-51] x-ray diffraction,[52-54] transmission electron microscopy[55-64] and others[65] all demonstrate the complexity of devitrification reactions in metallic glasses. Although some of these studies are interesting scientific investigations, it must be remembered that each variation in composition and/or heating rate will produce a new set of metastable phases or new morphologies. Since amorphous alloys are essentially ruined whenever they crystallize, the technological value of this type of work is dubious.

While it is obvious to expect that amorphous alloys should crystallize upon heating, one would probably not expect significant changes to occur in metallic glass structure and properties below the crystallization temperature. Nevertheless, the literature repeatedly reports that amorphous alloys embrittle when annealed,[11,66-68] and that magnetic properties such as initial permeability[13,14,69] anisotropy,[3,14,70-75] and even Curie temperature[12,71,76-78] are modified by low temperature anneals.

Explanations of annealing behavior fall into several categories. Relief of internal stresses is probably the most often cited.[5,79,80] The main idea is that internal stresses are quenched into the alloy during fabrication; low temperature annealing relieves these stresses by allowing small atomic displacements. Compositional short-range ordering has been hypothesized to account for changes in Curie

temperature and magnetic anisotropy.[12,77] Topological short range ordering,[77] domain wall stabilization,[75] and structural relaxations[39,78] are all cited to explain some aspects of annealing behavior. The confusion implied by this multiplicity of models seems to arise from the difficulty in obtaining atomic scale information from small regions of amorphous materials.

This work presents the results of an investigation of the annealing behavior of a high permeability, zero magnetostriction Co|Fe|Si|B amorphous alloy. Conventional, high resolution, and Lorentz electron microscopy, in conjunction with bulk magnetization data, are used to obtain an overall understanding of atomic mechanisms of annealing in this amorphous alloy. This study is strictly limited to the particular alloy $Co_{71.4}Fe_{4.6}Si_{9.6}B_{14.4}$, prepared by roller quenching, but comparison with the literature indicates that many of the ideas presented here have broader applicability. It is hoped that this study may be useful for explaining the response of amorphous alloys to annealing.

II. EXPERIMENTAL

The amorphous alloy chosen for this study had a nominal composition $Co_{71.4}Fe_{4.6}Si_{9.6}B_{14}$. It was prepared by TDK Corporation using a commercial roller quenching techniques in the form of a continuous ribbon, 1cm wide and 40μm thick.

Magnetization curves obtained using an integrating fluxmeter were used to determine the saturation magnetization, B_S, the remanent magnetization, B_R and the coercive force, Hc. Effective initial permeability, μ_{10}, was measured in a 10mOe field at 1kHz. Magnetostriction, λ, was measured qualitatively by observing changes in the magnetization curves under the influence of an applied mechanical stress. The anisotropy, K, was taken as the difference between the area under the magnetization curves for magnetization parallel to the easiest and hardest directions in the material. All measurements were made at room temperature following thermal treatments in argon atmospheres.

Electron transparent specimens for transmission electron microscopy (TEM) were prepared using conventional electropolishing techniques. 3mm discs were spark-cut from the original roller-quenched ribbons. In order to obtain a smooth surface for electropolishing, the discs were ground on 600 grit emery paper until the surface layer was removed. Electropolishing was done using a standard Fischione twin-jet polishing apparatus with an electrolyte of:

6 volume percent	60% solution of perchloric acid
31 volume percent	glycerol and
63 volume percent	glacial acetic acid.

The electrolytic cell operated at an applied potential of 45V and a current of 30mA. Since hand grinding thinned the discs to approximately 20 μm, performation normally occurred after only 45 seconds.

The foils were immediately removed, washed in ethanol, dried and stored in vacuum.

Conventional and Lorentz electron microscopy were done using a Philips EM301 transmission electron microscope. A Philips P400 analytical electron microscope was used for microanalysis of crystallized phases. Structural images of amorphous material were formed using a JEOL 200CX high resolution TEM operated at 200kV and analyzed for periodicities using a light optical diffractometer.[81]

III. RESULTS

The amorphous alloy $Co_{71.4}Fe_{4.6}Si_{9.6}B_{14.4}$ has been designed for essentially zero magnetostriction ($|\lambda| < 1 \times 10^{-6}$) and high permeability (μ_{10} = 11,000, as quenched). The Co to Fe ratio has been chosen to minimize magnetostriction; the Si and B have been added to ease glass formation and to increase thermal stability. Since this alloy exhibits negligible magnetostriction, elastic effects can be essentially decoupled from magnetic behavior. This results in significant simplification in data analysis. Other material parameters include 1) coercive force (H_c = 0.035 Oe, as quenched), 2) crystallization temperature at 5°C per minute heating rate (T_{cry} = 488°C) and 3) Curie temperature (T_c = 457°C).

The variations of magnetic properties with thermal treatments are presented in Figures 1-5. Figure 1 presents μ_{10} as a function of annealing temperature, T_a; T_c and T_{cry} have been noted in this figure in order to demonstrate that μ_{10} varies radically due to annealing below both transition temperatures. H_c, K, and B_R appear as functions of T_a in Figures 2, 3, and 4 respectively. It should be noted that data in Figures 1-4 are consistent; an increase in K is accompanied by an increase in H_c and a decrease in μ_{10}. The low K at T_a = 460°C is accompanied by a reduced remanence, B_R/B_S, approaching 0.5, characteristic of isotropic materials. The variation of μ_{10} with annealing time at 460°C appears in Figure 5. This illustrates the critical time dependence of annealing behavior near T_{cry}. The maximum μ_{10} of Figure 5 is higher than μ_{10} for the as-quenched state (see Figure 1), indicating that carefully designed and controlled heat treatments can improve magnetic properties of this alloy.

TEM images of the amorphous phase produced no contrast in conventional bright field (BF) and dark field (DF) imaging conditions; selected area diffraction (SAD) produced only diffuse ring patterns. Figure 6 is an example of BF and DF images along with the SAD pattern taken from the amorphous alloy. Figure 7 is an example of the crystal morphology which forms by a nucleation and growth process when this alloy is heated to T_{cry}. Analysis of SAD patterns show that these crystals have hexagonal symmetry. This is reasonable for this alloy since it is predominantly cobalt.[82] X-ray microanalyses gave no evidence of significant compositional differences between crystal and matrix.

High resolution TEM images taken at -800Å defocus of the amorphous alloy in the as-quenched and 300°C annealed conditions are shown in Figures 8 and 9 respectively. The corresponding SAD patterns and light optical diffraction patterns are included in the insets. Light optical diffractometry is used to detect and measure periodicities contained in the image negative.[83] The absence of any distinct bright spots in the light optical diffractograms reflects the lack of periodic structures in the images. In other words, the light optical diffractogram confirms the visual impression that the image represents a non-periodic structure. Light optical diffractograms from amorphous materials can be used to determine the contrast transfer characteristics of the microscope.[84,85,86] The light optical diffractograms have been presented here to establish the condition of the microscope when these images were formed. Further analysis of the light optical diffractograms could produce more information about the JEOL 200 CX microscope, but this information would fall outside the scope of this thesis and will therefore not be presented here.

Lorentz electron microscopy (LEM) techniques exploit the deflection which the electrons undergo while passing through magnetic foils in order to obtain images of magnetic domain structures. The several techniques for magnetic contrast are well described in the standard texts on TEM.[87-89] The defocused (Fresnel) mode of Lorentz imaging is the only one practicable for amorphous specimens. In order to obtain the highest possible resolution of magnetic structures, it is imperative that the specimen illumination be parallel.[90] Practically, this requires that the microscope condensor system be defocused; the resulting low intensities require image exposure times in excess of 5 minutes.

Specifically, for the Philips EM301, excellent defocused LEM images can be obtained by 1) shutting off the objective lens and switching focussing controls to the diffraction lens by making use of the "LM" image mode, and 2) by completely defocussing both condensors and exposing for the order of 8 minutes. The highest possible magnification which can be obtained using this method on this instrument is only 4500X. This presents no real limitation because resolvable magnetic structures can easily be recorded in the photographic emulsion at this magnification.

Figure 10 is an example of a typical LEM image of magnetic structures in thin foils of this amorphous alloy. The most prominent feature of this image is the cross-tie domain wall which extends across the image. Cross-tie domain configurations represent an intermediate form between Bloch and Neél walls and only appear in anisotropic thin foils.[91] An interpretation of the magnetic orientations in the neighborhood of a cross-tie wall is provided in Figure 11. Closer examination of Figure 10 reveals the presence of small scale contrast fluctuations throughout

the background. Similar fluctuations occur in polycrystalline thin films and are called "magnetization ripple".[92] Magnetization ripple is attributed to the presence of local anisotropies in the film.[92-94] Because of the image formation process, ripple always lies perpendicular to the local magnetization orientation.[92] The presence of ripple here is an indication of localized anisotropies in this metallic glass.

A special specimen stage was used to confirm that the contrast fluctuations were truly due to magnetization ripple. By applying a small magnetic field to the specimen during observation of magnetic structures, it was possible to cause motion of both the magnetic domain walls and the ripples. Because of instabilities in the power supply for the stage, it was impossible to take photographs of the domain walls when any field was applied.

As an indication of the sensitivity of magnetic structures to atomic structures, Lorentz images were obtained from a foil which had been partly crystallized. The domain walls are seen in Figure 12 to interact strongly with crystals in the amorphous matrix. Because of the lack of chemical differences between crystals and matrix, this interaction must be attributed to magnetocrystalline anisotropy in the crystals.

In an attempt to correlate magnetic structures (domain walls and ripples) with magnetization data, specimens were annealed ex situ and observed using LEM. Unfortunately, it was impossible to detect differences between specimens annealed at different temperatures. In situ heating experiments proved more fruitful. Although no changes in magnetic structures were observed while heating from room temperature to 300°C, at higher temperatures the magnetization ripple tended to align

perpendicular to the local magnetization direction. Figure 13 demonstrates this behavior. In Figure 13a, taken at room temperature, the ripple appears to be independent of the magnetization in the domains. The ripples in Figure 13b, taken with a foil temperature of approximately 450^{o}C are aligned radially about the wall junction. The alignment of ripples at 450^{o}C is accompanied by corresponding changes in the configuration of the Bloch domain walls. Figure 14 shows how the Bloch walls move during heating to assume a configuration which is nearer to equilibrium. The situation observed in Figure 14b, taken at approximately 450^{o}C, evolved from that of Figure 14a due to heating.

IV. DISCUSSION

Any discussion of structure property relationships in a noncrystalline material must necessarily be somewhat nebulous. Lacking the regularity of a crystal lattice, an amorphous material has the freedom to assume a continuous spectrum of atomic configurations. In comparison, the configurations available to crystalline materials are severely limited. The variety of structures available to an amorphous material is reflected in a similar variety of physical properties. Although this variety of physical properties may, at some future date, prove useful for materials design, at present there is no experimental technique which can define an amorphous structure uniquely, and any description of amorphous behavior is typically clouded by many qualitative and poorly defined expressions. Unhappily, this discussion will probably fall into this pattern.

This discussion will be divided into two essentially different areas. First of all, it will be necessary to evaluate the utility of conventional and high resolution TEM techniques when applied to metallic glasses. It is important to determine how much credence can be given to conclusions obtained from HREM images of metallic glasses. The second part of this discussion will be directed toward the more practical problem of annealing behavior of metallic glasses. It will be possible to hypothesize a mechanism for annealing solely on the basis of magnetic measurements. After a discussion of image formation and interpretation of high resolution LEM images, it will be shown that the LEM technique can be used to confirm the hypothesized annealing mechanism.

A. Conventional and High Resolution TEM

The application of TEM techniques to amorphous materials has been discussed in the literature,[86] and no attempt will be made to treat the subject extensively here. It will suffice to say that to detect small regions in an amorphous matrix, TEM has an inherent advantage over x-ray diffraciton techniques because it does not average information taken from large areas of the specimen. Several excellent studies of metallic glass structures using x-ray diffraction techniques have concluded that metallic glasses are indeed amorphous.[6-8] By themselves, these studies do not necessarily preclude the presence of small regions of crystalline material in the amorphous matrix since diffraction information from crystalline regions could conceivably be lost in the diffuse scatter from the disordered regions. The TEM images shown in Figure 6 ostensibly complement the diffraction studies by obtaining information from much smaller regions of material. One may conclude from these studies that metallic glasses are indeed amorphous to the limits of the techniques.

The high resolution electron microscopy techniques, which attempt to detect crystallinity in glassy materials by forming real space images of lattice periodicities are of extremely limited value for disordered metallic materials. As pointed out by Krivanek,[86] the high resolution technique should theoretically be able to produce more information about amorphous materials than diffraction techniques because of its ability to obtain phase information, not just intensity information. This is good in principle, but the experimental requirements all but prohibit application to metallic glasses. The most restrictive requirement is that the specimen be extremely thin. It is

necessary that the crystal planes responsible for any lattice fringe image extend through the depth of the foil. If the crystals had not been detectable using diffraction contrast techniques, they would have to have been very small. To detect these crystals would require that the foil be thinner than the diameter of the crystals. In this regime, surface effects are obviously very important. Surfaces of metallic glasses have not been well-characterized, but it would seem likely that the atomic configurations near surfaces be significantly different from those in the bulk. Oxidation and surface relaxation effects can both be present on surfaces of non-equilibrium metallic materials. If crystals were detected by HREM only, it is doubtful that they would be representative of the bulk.

Recently Gaskell, et al.[9] have published HREM images of evaporated films of Pd_4Si taken on the Cambridge University atomic resolution microscope. This work shows the sensitivity of the technique to specimen thickness; fringes were visible only if the foil was $\leq 25\text{Å}$ thick. In light of the previous arguments, it is doubtful whether these HREM images provide any information about bulk structures of amorphous Pd_4Si or metallic glasses in general.

The HREM images presented in Figures 8 and 9 serve to support other evidence which has concluded that metallic glasses are non-crystalline. The failure of the HREM to detect any changes in structure after $300^{\circ}C$ anneal does not disprove the hypothesis to be advanced in later parts of this thesis, that magnetic hardening during annealing arises from a directionality of ferromagnetic atoms. This directionality results in localized magnetic anisotropy, but it does not involve any periodicities which would be detectable with HREM.

Possibly the most convincing evidence for a lack of crystallinity in metallic glasses is the complete agreement of all investigators using many different experimental techniques. Bulk calorimetry experiments,[37-39] and magnetic property measurements[30,35,36] all agree that there is no reason to suspect metallic glasses are microcrystalline. Especially convincing is the report[75] that magnetic annealing effects are reversible when the annealing temperature is cycled above and below T_c. If there were crystallites in the glass, it is inconceivable that they would be made to grow at low temperatures and then to defy the driving force for crystal growth by shrinking at high temperatures. It seems safe to conclude that it is possible to fabricate alloys which can best be described as structurally amorphous.

B. Annealing Behavior

1. Explanation of Annealing Behavior. The response during annealing of the amorphous alloy $Co_{71.4}Fe_{4.6}Si_{9.6}B_{14.4}$, as reported in Figures1-5, can be divided into three regimes. For T_a below 400°C, μ_{10} decreases while H_c and K increase. In the range $400°C < T_a < T_{cry}$, the behavior reverses and the alloy regains some or all of its original magnetic softness. Above T_{cry} the alloy magnetically hardens rapidly and irreversibly. This section presents a detailed explanation of the entire spectrum of annealing behavior of annealing behavior in terms of atomic structures.

Low temperature aging treatments are characterized by two phenomena. The internal magnetic field or "Weiss molecular field"[96] of this ferromagnetic material acts to align atoms in such away that an anisotropy is generated in the material. Opposing this is the stress relaxation phenomenon which has received a great deal of attention in the literature.[5,80] Of these two, the first seems to be of much greater importance for this alloy.

It was recognized quite early in the history of metallic glasses that magnetic field annealing was effective in inducing a magnetic anisotropy in a metallic glass without causing crystallization.[2,3] In a crystalline material, magnetic anisotropy results from a coupling between atomic magnetic moments and the crystalline lattice. The same effect is possible in an amorphous material. The ability of some rare earth-transition metal amorphous alloys to sustain magnetic bubbles[97] is evidence of an interaction between magnetic moments and local atomic environment. Evidently, magnetic field annealing must somehow produce anisotropic atomic environments. Mechanisms which have been proposed to account for magnetic field annealing have generally involved some

degree of pair ordering.[98] Under the influence of the internal magnetic field and thermal vibrations, atoms rearrange to produce a statistically higher probability of finding nearest neighbor ferromagnetic atoms along one direction than along another. In other words, the atomic pair distribution function for the ferromagnetic components is no longer spherically symmetric. In the case of a four component system it is easy to see how this could occur. Even in a two component system such as $Fe_{80}B_{20}$, pair ordering occurs, although the effect is lessened.[1] The pair ordering mechanism requires short-range diffusion. As in all glassy materials, diffusion occurs through an "excess free volume" mechanism.[99] Excess free volume refers to the regions in a glass having slightly reduced density and is the glass equivalent of a vacancy. Pair ordering is very similar to directional ordering which occurs in crystalline magnetic alloys[100] and the maximum induced anisotropy is of the same magnitude.[1] The pair ordering mechanism adequately explains the anisotropy which can be induced during magnetic field annealing.

Despite the large number of investigations into annealing behavior in metallic glasses, the literature seems to have overlooked the fact that the Weiss molecular field exists in all ferromagnets below the Curie temperature, even in the absence of an applied field. In fact, the strength of this internal field is larger than any field which can be generated in the laboratory.[96] During magnetic field annealing, the applied field only serves to saturate the material so that the induced anisotropy is uniform throughout the material and may be detected on a macroscopic scale. The strength of the field at any atom is probably not changed significantly under the presence of an applied field, but its direction may be changed In the absence of the applied field, the material demagnetizes by breaking up into domains

in order to reduce magnetostatic energy. Annealing the demagnetized material will evidently, then, induce anisotropy which varies in direction from domain to domain. Therefore, any annealing treatment on metallic glasses below their Curie temperature will be effectively a magnetic field anneal whose effects are not uniform throughout the material. Any material which is responsive to magnetic field annealing will behave similarly when annealed below T_c. This effect has been termed "domain wall stabilization" because the induced anisotropy increases the barrier to magnetic moment rotation. A material with stabilized domain walls will exhibit a "wasp waist", or constricted, hysteresis loop like the commercial perminvars.[101] This effect was observed in this,[102] and similar,[75] amorphous alloys. The absence of magnetocrystalline anisotropy in metallic glasses allows domain wall stabilization to occur in any orientation and domain configuration.

The presence of magnetization ripples in an amorphous alloy, as shown in Figure 10, complicates matters further. The ripples are indicative of the fluctuations in anisotropy on a scale much smaller than that of the magnetic domains.[92] The origin of these fluctuations in the as-quenched state is not yet clear, although, as Shiiki et al.[103] have suggested, it is probably related to clustering in the melt or some other aspect of the fabrication process.

Fluctuations in anisotropy can be of two kinds. If pair ordering is present, anisotropy due to coupling of the atomic magnetic moment to the local environment (magneto- "crystalline" anisotropy) occurs. If there are large deviations from average composition, the local magnetostriction constant will be non-zero and strain magnetostriction coupling will produce anisotropy. When an alloy containing fluctuations is annealed, the local anisotropy and the local internal

field act to effectively strengthen the local anisotropy.

The annealing response of $Co_{71.4}Fe_{4.6}Si_{9.6}B_{14.4}$ for $T_a < 400^oC$ can be explained in terms of this domain wall stabilization, or "magnetic self anneal", mechanism. Initial permeability is a measure of a material's resistance to the reversible part of magnetization rotation. If the local anisotropy throughout this alloy is increased, the resistance to the smallest degree of rotation is increased. This produces the decrease in μ_{10} which occurs during anneals below 400^oC. The bulk anisotropy, K, as reported in Figure 3, measures the differences in the energy required to saturate the alloy along different directions. The remanence (Figure 4) is nearly constant in this regime at a non-zero value. This implies that all possible directions of magnetization are not equally represented. Thus, the anisotropy induced on a local scale will not equally represent all directions. K is an average of local anisotropies; it will not average to zero. As the strength of local anisotropies increase, so does K. The remanence itself may have largely originated from the fact that the material is in the form of a thin ribbon. This is a case where-shape anisotropy, which is a magnetostatic effect, induces anisotropic coupling between a atomic moment and its environment. Coercive force, H_c, is essentially a measure of the difficulty of producing irreversible magnetization rotations. Motion of domain walls through a material which has a fluctuating local anisotropy will be difficult. Evidently, increasing the strength of the anisotropy will increase the difficulty of domain wall motion, and H_c will increase. This agrees well with Figure 2, but Luborsky et. al.[3], have reported the opposite behavior, namely, that the coercivity decreases with magnetic field annealing. The distinction here is that magnetic field annealing eliminates local anisotropy and replaces it with uniform anisotropy. Uniform anisotropy presents less resistance to irreversible

domain wall motion. Domain wall stabilization, therefore, simply and completely explains low temperature annealing behavior.

Confusion regarding annealing behavior exists in the literature because of the failure to recognize the effects of the internal magnetic field. This is evident in the attempts by Luborsky and Walter[5] and Chen and Egami[12] to understand the kinetics of "stress relaxation" and "compositional short range ordering" without recognizing that atomic motions will be influenced by the molecular field. In these papers, and possibly others, complex temperature dependences of annealing phenomena have been reported. Typically what occurs is that the annealing response as measured by stress relaxation or Curie temperature changes is essentially zero at high annealing temperatures. The fact that this Curie temperature coincides with the temperature where the annealing response goes to zero seems to indicate that the magnetic effects are important. This is further evidence for the domain wall stabilization mechanisms.

Stress relaxation is commonly believed to occur during low temperature annealing of metallic glasses. Stresses quenched in during fabrication are dissipated by short-range atomic motions. Experiments using artificially applied stresses have shown[5] that stresses can indeed be relieved during low temperature annealing. It is, however, not explained how stresses of this magnitude can be produced during splat quenching. Whether or not large stresses actually exist is probably not important for this zero magnetostrictive alloy.

Throughout the temperature range $T_a < T_{cry}$, there is a competition between the ordering tendencies of the internal field and the disordering tendencies of thermal vibrations. As discussed above, magnetic alignment predominates for $T_a < 400^oC$. Above 400^oC the strength of the internal field decreases to zero at T_c and the

amplitude of thermal vibrations increases. The result is that the effect of magnetic properties is reversed. Above T_c, the internal field is absent and thermal disordering produces a nearly isotropic material. This is reflected by the magnetic properties reported in Figures 1-5.

If time and temperature are sufficiently large, metallic glasses begin to crystallize by homogeneous nucleation and growth. The presence of crystalline phases effectively ruins the excellent soft magnetic properties of metallic glasses. This can be seen in the dramatic drop in μ_{10} and the rise in H_c and K at $T_a < T_{cry}$. Magneto crystalline anisotropy and strain magnetostriction coupling effects cause magnetic domain walls to be pinned by the crystalline phase and the alloy becomes magnetically hard.

2. Lorentz Electron Microscopy. To confirm the analysis of the annealing behavior presented above, this investigation has been forced to rely on an experimental technique which can only obtain indirect structural information on a microscopic scale. Up to this point the analysis of annealing behavior has been built up on magnetic property measurements and a general knowledge of ferromagnetic materials. Thus the analysis has relied on indirect information averaged over many atoms. Of course, it is desirable to have more direct structural information. X-ray diffraction techniques produce direct structural information, but it is averaged over a macroscopic specimen; TEM obtains structural information on a microscopic scale. The literature contains many X-ray investigations, none of which have been effective in explaining annealing behavior. In the first part of the discussion above, TEM has also been shown to be ineffective. Lorentz electron microscopy (LEM) is used to obtain information about magnetic, as opposed to atomic, microstructures. As such, it produces indirect information on atomic structures on a microscopic scale. This investigation has been forced to resort to LEM to confirm the analysis as presented above.

This section discusses the LEM images in terms of the above analysis. The results of the LEM experiments go a long way toward confirming the analysis of the magnetization data. At the outset, it should be noted that the information in a LEM image is limited in scope and indirect in nature. For this reason, the LEM images, presented in this thesis can not be construed to be absolute proof of everything discussed above. Nevertheless, the agreement between the images and what would be predicted inspires a good deal of confidence.

The significance of Figure 10 has already been mentioned. The

cross-tie wall is an artifact of the thin film; the magnetization ripples are indicative of local fluctuations in magnetic anisotropy. The ripples in this as-quenched foil probably originate during the fabrication process.

The conclusions presented in the previous paragraph have been reached through straightforward application of the geometrical approach to LEM imaging. This is the approach taken by Fuller and Hale in their classic papers,[104-106] which contained the first published LEM images. This geometrical approach is the one which is normally treated in the standard texts on TEM.[87-89] The electron is treated as a charged particle and its deflection on passing through the magnetic field inside the TEM foil is used to form images representing domain walls. Since the deflection is small, it is necessary to focus the imaging lens above or below the specimen in order to record intensity differences. This is shown schematically in Figure 15. By suitable defocus, a cross-tie domain wall appears bright with dark bands; reversing focus reverses contrast. The width of the domain wall image is a geometrical function of the magnitude of the internal field, the thickness of the foil, the angular difference between magnetization orientations in adjacent domains, the thickness of the domain wall and the amount of defocus. The ripple appears because fluctuations in the direction of deflection produce the fluctuations in intensity. The obvious shortcoming of the geometrical approach is that there is no way to account for multiple fringes at the domain wall.

The geometrical approach to LEM imaging is useful for interpreting most LEM images, but it is not reliable near the limits of resolution of the technique, nor can it determine what those limits are. The wave-optical formulations originated by Boersch et al.[107,108]

and developed by Cohen,[90,109] Wade,[110] and Wohlleben[111-113] place LEM in the context of the phase contrast microscopy. Defocussing is then one of several techniques for obtaining phase contrast;[90] fringes at boundaries are a natural interference effect. Furthermore, Wohlleben's treatment[111] shows that, because the interaction of an electron with a magnetic field is relatively weak, the resolution of the technique will ultimately be limited by the uncertainty principle. In other words, reliable information can not be obtained which is finer than a certain fundamental limit. The resolution of the images presented in this thesis is near that limit.

The limitation imposed by the fundamental resolution limit of LEM is a severe drawback. Close examination of Figure 10 may lead to the conclusion that the fluctuations in anisotropy have a characteristic periodicity of approximately 1000Å and that there are no fluctuations on a finer scale. The first clue that this may not be true is that the periodicity of the ripples seems to be the same as that of the fringes at the cross-tie wall. According to Wohlleben,[111] the width of the fringes is the fundamental limit of resolution and the LEM technique cannot obtain any information about magnetic variations finer than that value. The fundamental limit of resolution is on the order of 10^3 atomic diameters. Further analysis of LEM images must be done in full cognizance of this fact.

In light of the limits of resolution of the LEM technique, it is not surprising that efforts to detect changes in magnetic structures after ex situ anneals failed. A series of experiments was conducted in which the alloy was furnace annealed below T_c and then thinned and examined using LEM. All images were qualitatively the same. Annealing in the demagnetized state should have stabilized the domain and ripple

structure which was present during annealing. However, this material is still magnetically very soft and handling and thinning processes would surely have rearranged the domains before they could be observed. What was observed was, almost universally, regions of material where the magnetic orientation was different from the direction of the local anisotropy. The increased anisotropy due to 300°C anneals may have had some effect on magnetic structure, but was not visible due to the poor resolution of LEM.

A series of hot stage experiments was done in order to observe the stabilization of magnetic structures directly. This technique circumvents the problem of domain rearrangement between stabilization and observation. In these experiments, the specimen was heated slowly while it was observed in LEM. THe domain wall configuration which is observed in an as-quenched specimen is probably the result of accidental rearrangements due to handling and thinning. Since the domain walls can be pinned by the anisotropy and the shape of the foil, the configuration is probably not in the ultimate equilibrium form. Heating up to 400°C stabilizes this configuration. A strengthening of anisotropy is the only effect below 400°C; no domain wall motion nor changes in ripple structure should occur. Experimentally, no changes in magnetic structures were observed. As the temperature of the specimen is raised near the Curie temperature the magnetic anisotropy is expected to decrease. As shown in Figure 13, this seems to occur; the ripple at room temperature (Figure 13a) becomes aligned perpendicular to the lines of magnetization at high temperatures (Figure 13b). The fact that the periodicity of the fluctuations becomes longer can be attributed to the decrease in strength of the anisotropy and consequent tendency toward a structure which is composed of a few well-defined domain walls and no

ripples. Thus, the ripples in Figure 13b are essentially collapsing to form a few small angle domain walls. Figure 14 is proof that the realignment and broadening of ripples in Figure 13 actually produces magnetic softening. The fact that the domain walls move during heating shows that the barriers to motion have been lowered. The coercivity (Figure 2) consequently decreases. The information in the LEM images agrees in all cases with the interpretation presented above.

Magnetization ripples in this alloy arise from localized anisotropy and are evidence that this alloy is not as magnetically soft as it should be. If they could be removed, significant improvements in magnetic softness could be realized. Annealing in the paramagnetic state ($T_c < T_a < T_{cry}$) is one way to do this. However, since T_c is very near T_{cry}, it is unlikely that the anisotropy can be totally removed without causing crystallization. It may, instead, prove easier to prevent the formation of ripples during preparation of the alloy. To do this, it is important to know whether the regions of local anisotropy form in the melt or during the solidification process. A systematic study of the preparation process may provide the answer, and the ripples may be finally eliminated. Therefore, further study of the preparation process is strongly recommended.

V. SUMMARY

Metallic glasses are known to be influenced by low temperature annealing treatments. Although the annealing behavior of many amorphous alloys has been investigated and reported, there exists no comprehensive understanding of the origins of annealing behavior. Thermal behavior of metallic glasses is of interest both from a scientific and from a technological viewpoint. This thesis presents the results of a study of annealing mechanisms for a single amorphous alloy $Co_{71.4}Fe_{4.6}Si_{9.6}B_{14.4}$. The fact that this alloy has essentially zero magnetostriction allows strain effects to be ignored and the analysis simplified.

LEM techniques have shown that, even in the as-quenched state, this amorphous alloy is not homogeneous and isotropic. This information has not been available from any other experimental technique. In particular, the currently available high resolution electron microscopy technique has been shown to be ineffective in characterizing inhomogeneities in this alloy, although it has indicated that this alloy is indeed non-crystalline. The inhomogeneities present in this alloy consist of small regions of ferromagnetic atoms. The extent of this ordering is never sufficient to produce any recognizable periodicities; this alloy must be characterized as amorphous. Nevertheless, the directionalities result in magnetic anisotropies.

Magnetic measurements on annealed specimens show dramatic changes during low temperature annealing. The alloy magnetically hardens for anneals below 300°C. Between 300°C and the crystallization temperature, this material magnetically softens, reaching a maximum softness for a ½ hour anneal between the Curie temperature, T_c, and the crystallization temperature T_{cry}. Above T_{cry}, the material rapidly and irreversibly hardens as crystals form in the amorphous matrix by homogeneous nucleation

and growth.

The low temperature annealing behavior ($T_a < T_c$) has been explained in terms of magnetic domain structure stabilization, although a small component of stress relaxation has not been excluded. During anneals below 300°C, the internal Weiss molecular field acts to align atoms by a pair ordering mechanism to produce local anisotropies within the magnetic domains in the material. The presence of inhomogenieties in the material causes the induced anisotropy to fluctuate on a much finer scale. The small scale anisotropies result in magnetic hardening. Above 400°C and below T_{cry}, thermal energy tends to disrupt the local anisotropies and the material magnetically softens.

Although it is a severely limited technique, Lorentz electron microscopy has been used to obtain information about microscopic magnetic structures. This information agrees with the analysis of annealing behavior in terms of localized anisotropy and domain wall stabilization.

To obtain the softest possible ferromagnetic material, the localized anisotropies must be removed from this material. Annealing in the paramagnetic state ($T_c < T_a < T_{cry}$) tends to do this, but it is doubtful that the process can be completed without causing some crystallization. If the anisotropies could be prevented from forming during fabrication, the necessity of post-fabrication anneals would be eliminated. To this end, this thesis recommends further analysis of fabrication techniques.

REFERENCES

1. C. D. Graham, Jr. and T.Egami, Ann. Rev. Mat. Sci. 8, 423 (1978).
2. B. S. Berry and W. C. Pritchet, Phys. Rev. Lett. 34, 1022 (1975).
3. F. E. Luborsky, J. J. Becker, and R. O. McCary, IEEE Trans. Magn. MAG-11, 1644 (1975).
4. J. L. Walter, D. G. Legrand and F. E. Luborsky, Mat. Sci. Eng. 29, 161 (1977).
5. F. E. Luborsky and J. L. Walter, Mat. Sci. Eng. 35, 255 (1978).
6. B. C. Giessen and C. N. J. Wagner, in Liquid Metals, S. J. Beer ed., (Marcel Dekker, N. Y., 1972), p. 633.
7. Y. Waseda, H. Okazaki, and T. Masumoto, J. Mat. Sci. 12, 1927 (1977).
8. G. S. Cargill III, in Solid State Physics, H. Ehrenreich, F. Seitz and D. Turnbull, eds., (Acad. Press, N.Y., 1975), p. 227.
9. P. H. Gaskell, D. J. Smith, C. D. J. Catto, and J. R. A. Cleaver, Nature 281, 465 (1979).
10. C. D. Graham, Jr., T. Egami, R. S. Williams, and Y. Takei, AIP Conf. Proc. #29, Magnetism and Magnetic Materials - 1975, Becker, Lander, and Rhyne, eds., p. 218.
11. C. A. Pampillo and D. E. Polk, Mat. Sci. Eng., 33, 275 (1978).
12. Y. N. Chen and T. Egami, J. Appl. Phys. 50, 7615 (1979).
13. O. Kohmoto, N. Yamaguchi, K. Ohya, H. Fujishima and T. Ojima, IEEE Trans. Magn. MAG-14, 949 (1978).
14. O. Kohmoto, H. Fujishima, and T. Ojima, IEEE Trans. Magn. MAG-16, 440 (1980).
15. P. Duwez, R. H. Willens, and R. C. Crewdson, J. Appl. Phys. 36, 2267 (1965).

16. C. C. Tsuei and P. Duwez, J. Appl. Phys. 37, 435 (1966).

17. A. I. Gubanov, Fiz. Tverd. Tela 2, 502 (1960).

18. R. Pond, Jr., and R. Maddin. Trans. AIME 245, 2475 (1969).

19. H. S. Chen and C. E. Miller, Rev. Sci. Instr. 41, 1237 (1970).

20. R. Hasegawa and R. C. O'Handley, J. Appl. Phys. 50, 1551 (1979).

21. T. Mizoguchi, AIP Conf. Proc. 34, Magnetism and Magnetic Materials - 1976, J. J. Becker and G. H. Lander, eds., p. 286.

22. T. Masumoto and R. Maddin, Mat. Sci. Eng. 19, 1 (1975).

23. T. Masumoto and K. Hashimoto, Ann. Rev. Mat. Sci. 8, 215 (1978).

24. F. E. Luborsky, IEEE Trans. Magn. MAG-14, 1008 (1978).

25. F. E. Luborsky, J. J. Becker, P. G. Frischmann, and L. A. Johnson, J. Appl. Phys. 49, 1769 (1978).

26. F. Spaepen and D. Turnbull in Second International Conference on Rapidly Quenched Metals, N. J. Grant and B. C. Giessen, eds., (MIT Press, Cambridge, 1976).

27. D. E. Polk and B. C. Giessen, in Metallic Glasses, J. J. Gilman and H. J. Leamy, eds., (ASM, Metals Park, 1977), p. 1.

28. R. C. O'Handley, M. C. Narasimhan, and M. O. Sullivan, J. Appl. Phys. 50, 1633 (1979).

29. R. C. O'Handley and M. C. Narasimhan, IEEE Trans. Magn. MAG-15, 970 (1979).

30. R. Hasegawa and R. Ray, J. Appl. Phys 49, 4174 (1978).

31. C. L. Chien and R. Hasegawa, J. Appl. Phys. 49, 1721 (1978).

32. R. Hasegawa, M. C. Narasimhan, and N. DeCristofaro, J. Appl. Phys. 49, 1712 (1978).

33. R. Hawegawa, R. C. O'Handley and L. I. Mendelsohn, AIP Conf. Proc. 34, Magnetism and Magnetic Materials - 1976, J. J. Becker and G. H. Lander, eds., p. 298.

34. R. C. O'Handley, L. I. Mendelsohn, R. Hasegawa, R. Ray, and S. Kavesh, J. Appl. Phys. 47, 4660 (1976).

35. S. Hatta, T. Egami, and C. D. Graham, Jr., Appl. Phys. Lett. 34, 113 (1979).

36. O. Kohmoto, K. Ohya, N. Yamaguchi. and T. Ojima, J. Appl. Phys. 50, 5054 (1979).

37. Y. Waseda and H. S. Chen, Phys. Stat. Sol. A49, 387 (1978).

38. F. E. Fujita, T. Masumoto, M. Kitaguchi, and M. Ura, Jap. J. Appl.. Phys. 16, 1734 (1977).

39. Y. Waseda and T. Egami, J. Mat. Sci. 14, 1249 (1979).

40. G. C. Chi and G. S. Cargill, III, Mat. Sci. Eng. 23, 155 (1976).

41. T. Egami, J. Appl. Phys. 50, 1564 (1979).

42. I. Vincze, D. S. Boudreaux, M. Tegze, Phys. Rev. B 19, 4896 (1979).

43. B. G. Lewis and H. A. Davis, Mat. Sci. Eng. 23, 179 (1976).

44. J. M. Vitek, J. B. Vander Sande and N. J. Grant, Acta Met. 23 163 (1976).

45. M. Doi, H. Okazaki, and T. Imura, in Rapidly Quenched Metals III, vol. 2, B. Cantor, ed., (The Metals Society, London, 1978), p. 372.

46. E. Coleman, Mat. Sci. Eng. 23, 161 (1976).

47. M. G. Scott and P. Ramachandrarao, Mat. Sci. Eng. 29, 137 (1977).

48. F. E. Luborsky, Mat. Sci. Eng. 28, 139 (1977).

49. F. E. Luborsky, H. H. Liebermann, Appl. Phys. Lett. 33, 233 (1978).

50. M. Matsuura, Solid State Communications 30, 231 (1979).

51. A. J. Kerns, D. E. Polk, R. Ray, B. C. Giessen, Mat. Sci. Eng. 38, 49 (1979).

52. M. Stubicar, E. Babic, D. Subasic, D. Pavuna, and Z. Marohnic, Stat. Sol. A44, 339 (1977).

53. I. Iwasaki and T. Masumoto, J. Mat. Sci. 13, 2171 (1978).

54. K. Osamura, K. Shibue, P. H. Shingu, Y. Murakami, J. Mat. Sci. 14, 945 (1979).

55. P. H. Shingu, K. Shimomura, K. Kobayashi and R. Ozaki, Mat. Sci. Eng. 23, 183 (1976).

56. J. L. Walter, P. Rao, E. F. Koch, and S. F. Bartram, Met. Trans. A 8A, 1141 (1977).

57. J. L. Walter, S. F. Bartram, and R. R. Russell, Met. Trans. A 9A, 803 (1978).

58. J. L. Walter, S. F. Bartram, and I. Mella, Mat. Sci. Eng. 36, 193 (1978).

59. E. Vafaei-Makhsoos, E. L. Thomas, and L. E. Toth, Met. Trans. A 9A, 1449 (1978).

60. U. Köster and U. Herold, Scripta Metall. 12, 75 (1978).

61. M. Von Heimendahl and G. Maussner, J. Mat. Sci. 14, 1238 (1979).

62. H. L. Yeh and R. Maddin, Met. Trans. A 10A, 771 (1979).

63. R. L. Freed and J. B. Vander Sande, Met. Trans. A 10A, 1621 (1979).

64. R. L. Freed and J. B. Vander Sande, Acta Met. 28, 103 (1980).

65. S. Tanigawa, K. Hinode, R. Nagai, K. Kanabe, M. Doyama, and N. Shiotani, Phys. Stat. Sol. A51, 249 (1979).

66. L. A. Davis, R. Ray, C. P.Chou, and R. C. O'Handley, Scripta Metall. 10, 541 (1976).

67. F. E. Luborsky and J. L. Walter, J. Appl. Phys. 47, 3648 (1976).

68. H. S. Chen, Scripta Metall. 11, 367 (1977).

69. K. I. Arai and N. Tsuya, IEEE Trans. Magn. MAG-13, 1550 (1977).

70. F. E. Luborsky and J. L. Walter, Mat. Sci. Eng. 28, 77 (1977).

71. H. H. Liebermann, C. D. Graham, Jr., and P. J. Flanders, IEEE Trans. Magn. MAG-13, 1541 (1977).

72. T. Miyazaki and M. Takahashi, Jap. J. Appl. Phys. 17, 1755 (1978).

73. I. C. Baianu, J. Patterson, and K. Rubinson, Mat. Sci. Eng. 40, 273 (1979).

74. H. Morita, H. Fujishima, and Y. Obi, Appl. Phys. 20, 125 (1979).

75. H. Fujimori, S. Ohta, T. Masamoto, and K. Nakamoto in Rapidly Quenched Metals, III, vol. 2, B. Cantor, ed., (The Metals Society, London, 1978), p. 232.

76. H. S. Chen, R. C. Sherwood, and E. M. Gyorgy, IEEE Trans. Magn. MAG-13, 1538 (1977).

77. T. Egami, Mat. Res. Bull. 13, 557 (1978).

78. A. L. Greer, and J. A. Leake, J. Non-Crys. Solids 33, 291 (1979).

79. G. C. Chi, H. S. Chen and C. E. Miller, J. Appl. Phys. 49, 1715 (1978).

80. F. E. Luborsky, J. L. Walter, and H. H. Liebermann, IEEE Trans. Magn. MAG-15, 909 (1979).

81. S. G. Lipson and H. Lipson, Optical Physics, (Cambridge Universith Press, London, 1969).

82. A. Inoue, T. Masumoto, M. Kikuchi, and T. Minemura, Sci. Rep. RITU. 27, 127 (1979).

83. R. Sinclair, R. Gronsky, and G. Thomas, Acta Met. 24, 789 (1976).

84. F. A. Lenz in Electron Microscopy in Materials Science, U. Valdre, ed., (Acad. Press, N. Y. and London (1971), p. 540.

85. F. Thon in Electron Microscopy in Materials Science, U. Valdre, ed., (Acad. Press, N. Y. and London 1971) p. 570.

86. O. L. Krivanek, Ph. D. Thesis, Cambridge University, 1975.

87. P. Hirsch, A. Howie, R.B. Nicholson, D. W. Pashley, M. J. Whelan, Electron Microscopy of Thin Crystals, 2nd ed., (Krieger, Huntington, N. Y. 1977), p. 388.

88. J. W.Edington, Practical Electron Microscopy in Materials Science, monograph 3, (Philips, Eindhoven, 1975), p. 84.

89. G. Thomas and M.J. Goringe, Transmission Electron Microscopy of Materials, (Wiley, N. Y. 1979), p. 185.

90. M. S. Cohen, J. Appl. Phys. 38, 4966 (1967).

91. P. J. Grundy and R. S. Tebble, Advan. Phys. 17, 153 (1968).

92. M. S. Cohen, in Handbook of Thin Film Technology, L. I. Maissel and R. Glang, eds., (McGraw-Hill, N. Y. 1970), chapter 17.

93. H. Hoffmann, IEEE Trans. Magn. MAG-4, 28 (1968).

94. K. J. Harte, J. Appl. Phys. 39, 1503 (1968).

95. D. Musser, C. L. Chien, F. E. Luborsky, and J. L. Walter, J. Appl. Phys. 50, 1571 (1979).

96. C. Kittel, Rev. Mod. Phys. 21, 541 (1949).

97. P. Chaudhari, J. J. Cuomo, and R. J. Gambino, IBM J. Res. Develop. 17, 66 (1973).

98. J. J. Becker, IEEE Trans. Magn. MAG-14, 938 (1978).

99. D. Turnbull and B.G. Bagley in Treatise on Solid State Chemistry, N. B. Hannay, ed., (Plenum, N. Y. 1975), p. 513.

100. S. Chikazumi and C. D. Graham, Jr., in Magnetism and Metallurgy, vol. 2, A. E. Berkowitz and E. E. Kneller, eds., (Acad. Press, N. Y. 1969), p. 577.

101. B. D. Cullity, Introduction to Magnetic Materials, (Addison-Wesley, Reading Mass. 1972), p. 368.

102. O. Kohmoto, Private Communication, Dec. 1979.

103. K. Shiiki, T. Watanabe, and M.Kudo, J. Appl. Phys. 50, 5419 (1979).

104. M. E. Hale, H. W. Fuller, and H. Rubinstein , J. Appl. Phys. 30, 789 (1959).

105. H. W. Fuller and M. E. Hale, J. Appl. Phys. 31, 238 (1960).

106. H. W. Fuller and M. E. Hale,J. Appl. Phys. 31, 1699 (1960).

107. H. Baersch, H.Hamisch, D. Wohlleben, and K. Grohmann, Zeitschrift für Physik 164, 55 (1961).

108. H. Boersch, H. Hamisch, K. Grohmann, and D. Wohlleben, Zeitschrift für Physik 167, 72 (1962).

109. M. S. Cohen, J. Appl. Phys. 39, 1149 (1968).

110. R. H. Wade, in Electron Microscopy in Materials Science, U. Valdre, ed., (Acad. Press, N. Y. and London 1971), p. 680.

111. D. Wohlleben, J. Appl. Phys. 38, 3341 (1967).

112. D. Wohlleben, J. Appl. Phys. 41, 1344 (1970).

113. D. Wohlleben, in Electron Microscopy in Materials Science, U. Valdre, ed., (Acad. Press, N.Y. and London 1971), p. 712.

FIGURE CAPTIONS

Figure 1 Variation of initial permeability, μ_{10}, with annealing temperature, T_a. (1 hour anneals).

Figure 2 Variation of coercive force, H_c, with annealing temperature.

Figure 3 Variation of bulk anisotropy K, with annealing temperature.

Figure 4 Variation of remanence, B_R (or reduced remanence B_R/B_S) with annealing temperature.

Figure 5 Variation of initial permeability, μ_{10}, with time at T_a = 460°C.

Figure 6 (A) Conventional bright field and (B) centered dark field (on the diffuse ring) transmission electron micrographs of the amorphous alloy in the as-quenched state. The corresponding selected area diffraction pattern appears as an inset.

Figure 7 Bright field and selected area diffraction pattern from partially crystallized Co/Fe/Si/B alloy.

Figure 8 High resolution structural image of the as-quenched amorphous alloy. The insets are the selected area diffraction pattern (lower left) and light optical diffraction pattern (upper right). (~800Å defocus) (Courtesy JEOL Corporation).

Figure 9 High resolution structural image of the amorphous alloy after 300°C anneal. The insets are the selected area diffraction pattern (lower left) and the light optical diffraction pattern (upper right). (-800Å defocus). (Courtesy JEOL Corporation)

Figure 10 Lorentz electron micrograph of a typical cross-tie domain wall in the as-quenched amorphous alloy. The cross-tie wall (A - A) is marked by Neél segments at (B) and Bloch lines at

(C). The contrast fluctuations in the background are due to magnetization ripples.

Figure 11 Schematic illustration of the magnetization orientations (arrows) near the cross-tie wall.

Figure 12 Lorentz electron microscopy image of Bloch walls (A - A) in the presence of a few isolated crystals (B) in the amorphous matrix.

Figure 13 Behavior of magnetization ripples during heating in situ. The ripples in the as-quenched state (a) align radially about the Bloch wall junction in (B) at 450°C.

Figure 14 Behavior of domain walls during heating in situ. Because of the decrease in anisotropy which occurs while heating from room temperature to 450°C, the domain wall configuration in (a) is free to move to that in (b).

Figure 15 Schematic illustration of Lorencz electron microscopy image contrast formation in the geometrical approach. Electrons in the incident beam are deflected by the discontinuous magnetic fields in th demagnetized specimen. If the image plane is moved below the specimen by defocussing, the domain walls at A and B will appear bright (intensity overlap) and dark (no intensity), respectively. Reversing defocus reverses contrast.

FIGURES

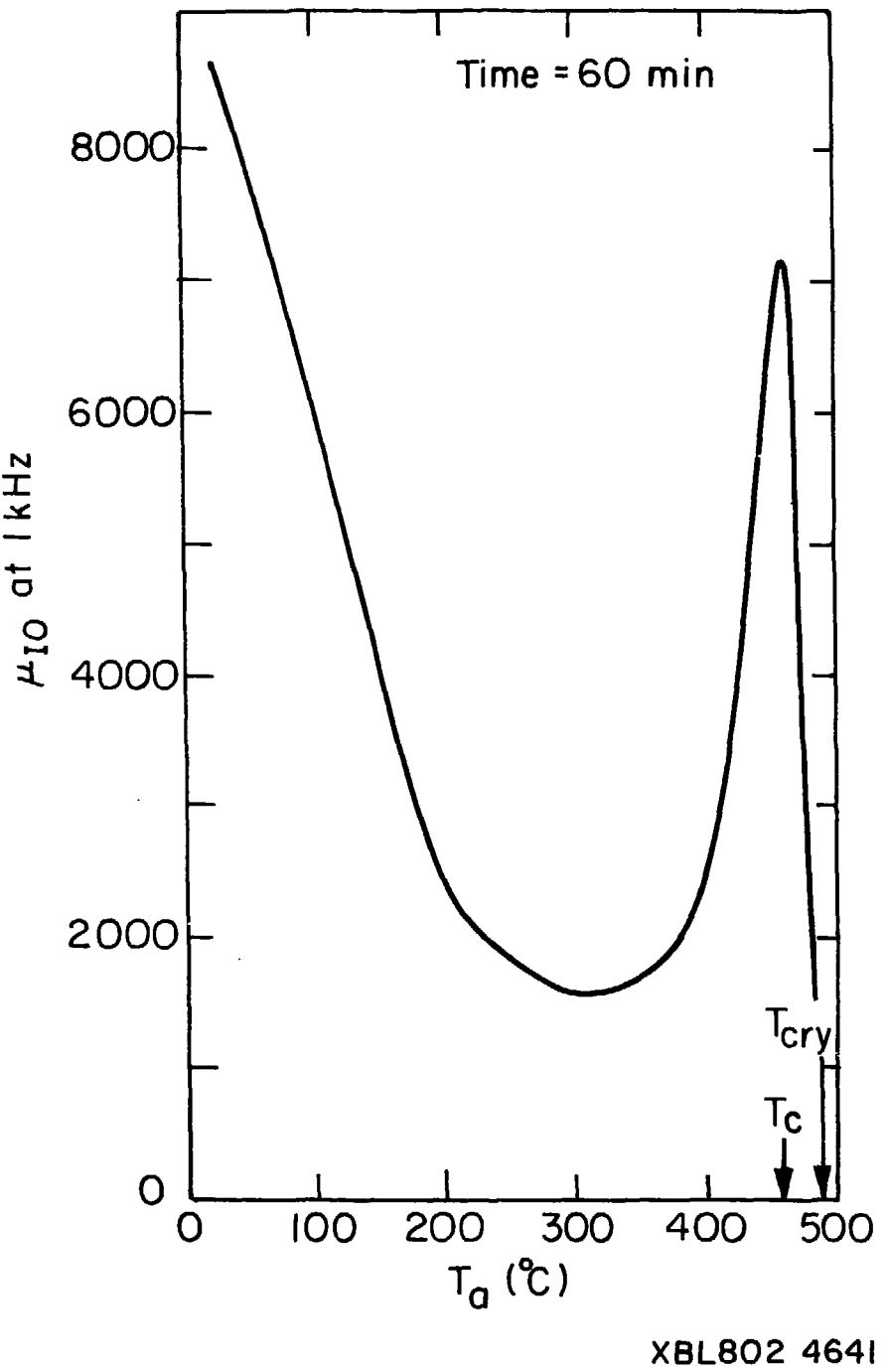
Time = 60 min
8000
6000
4000
2000
0
μ_{10} at 1 kHz
0
100
200
300
400
500
T_a (°C)
T_{cry}
T_c
XBL802 4641

Fig. 1

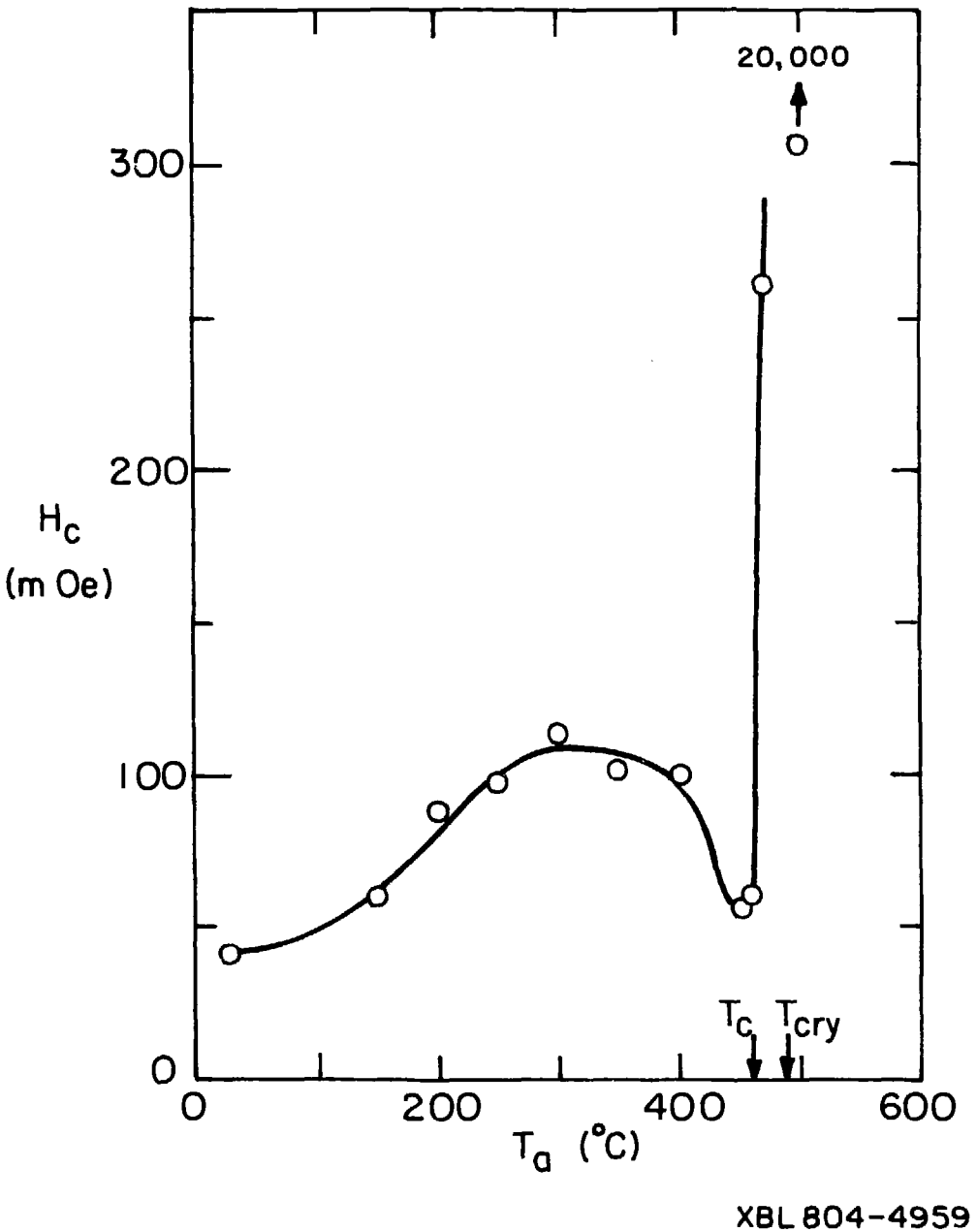

Fig. 2

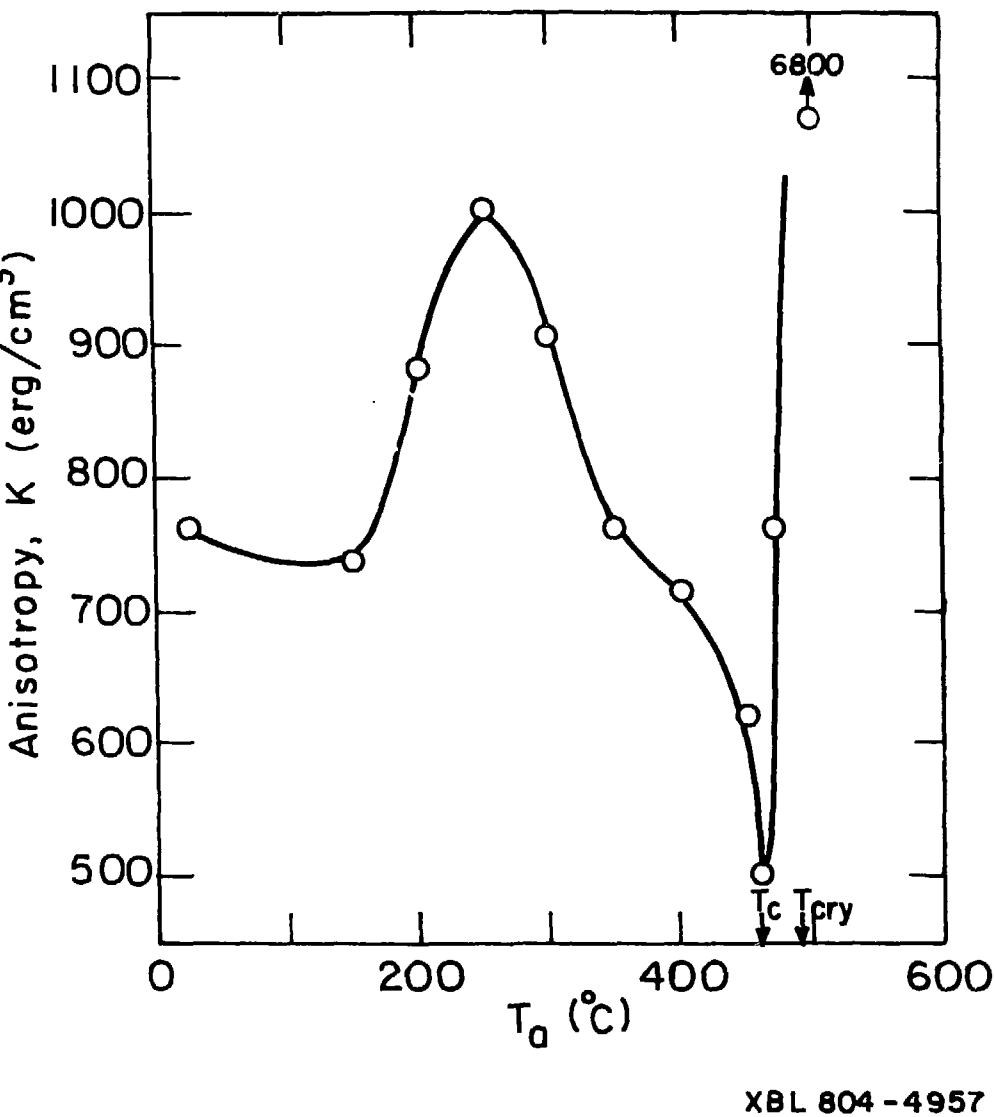
6800
1100
1000
900
800
700
600
500
Anisotropy, K (erg/cm³)
0
200
400
600
Ta (°C)
Tc
Tcry
XBL 804-4957

Fig. 3

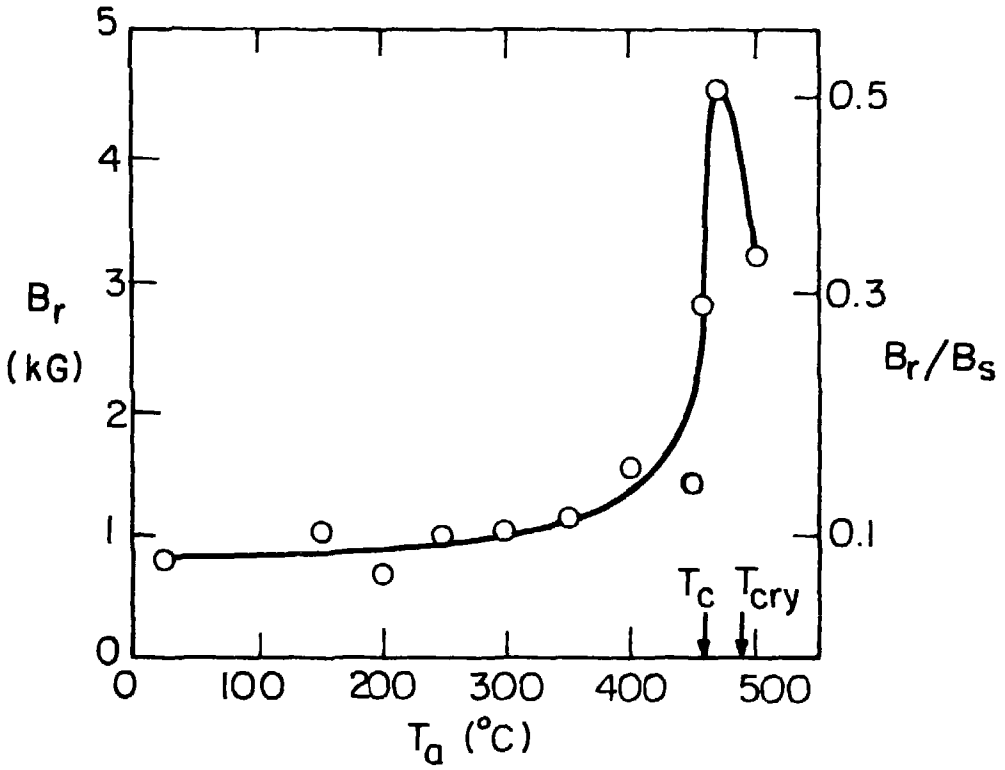

XBL 804-4956

Fig. 4

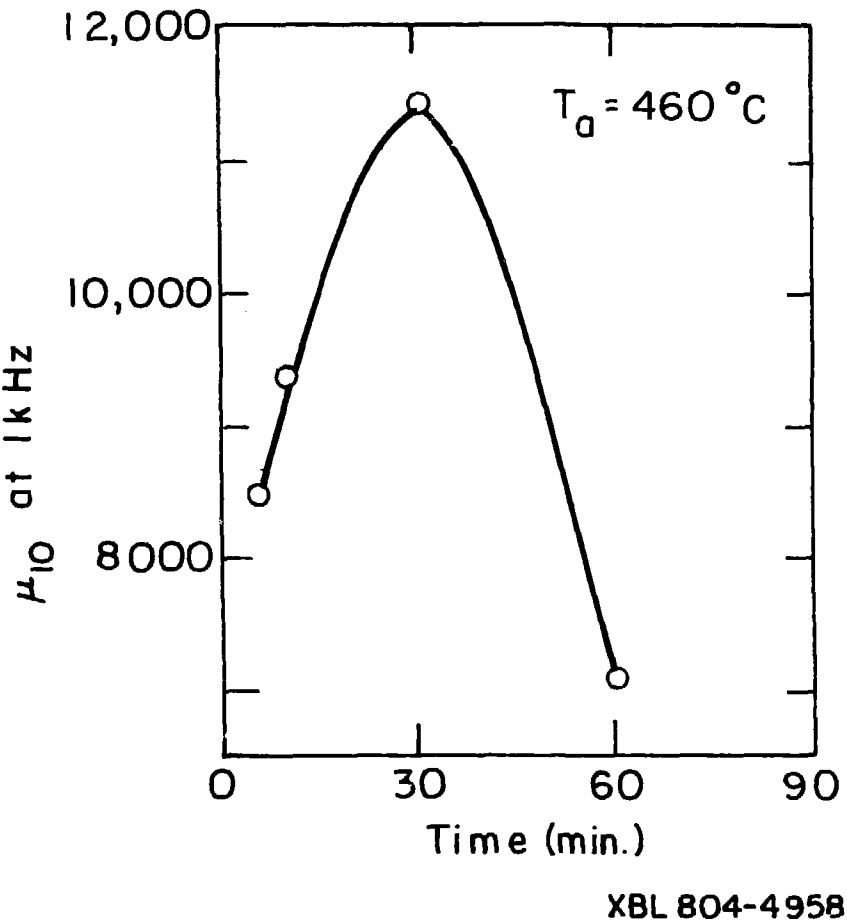
12,000
10,000
8000
μ_{10} at 1 kHz
T_a = 460 °C
0
30
60
90
Time (min.)
XBL 804-4958

Fig. 5

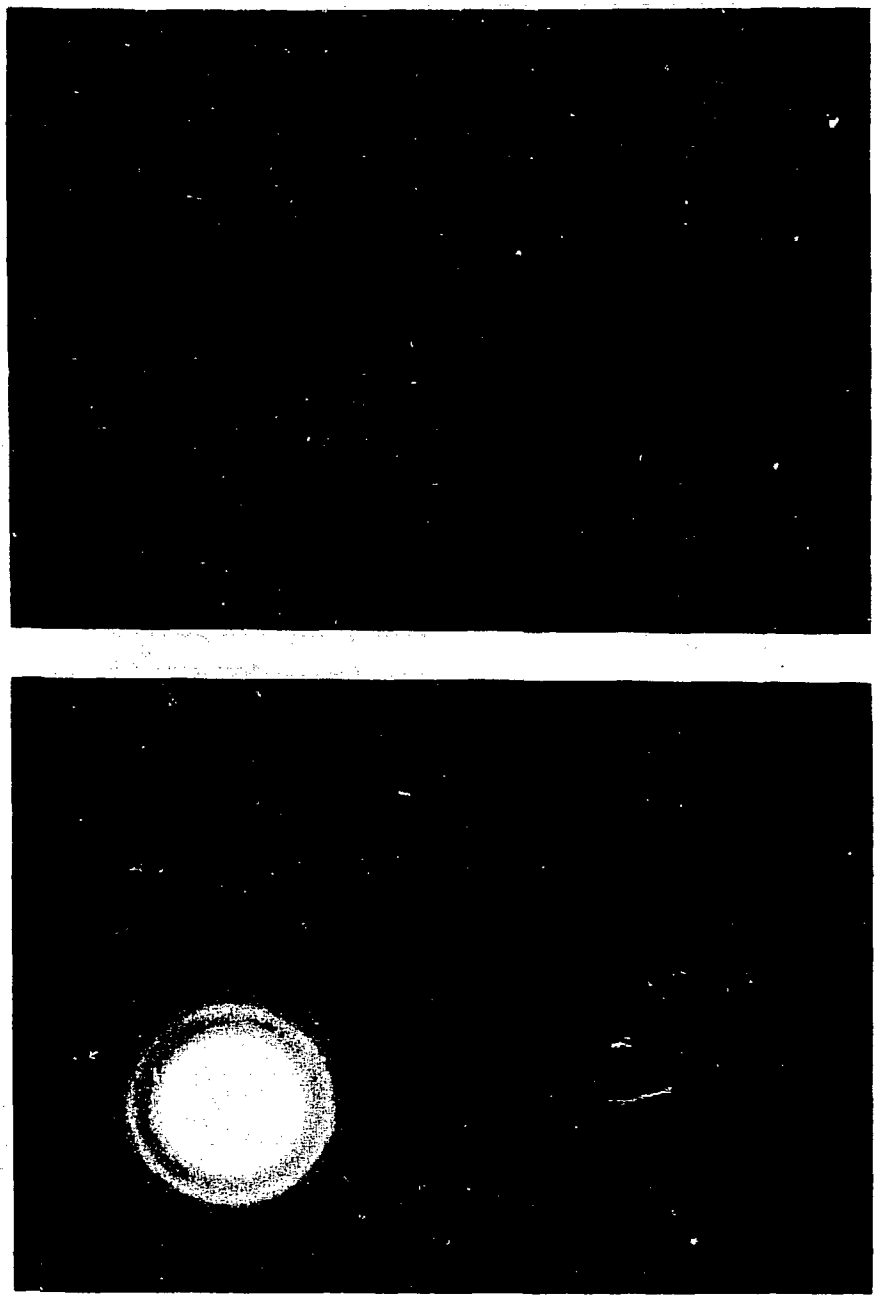

XBB 805 6334

Fig. 6

XBB 804 4576

Fig. 7

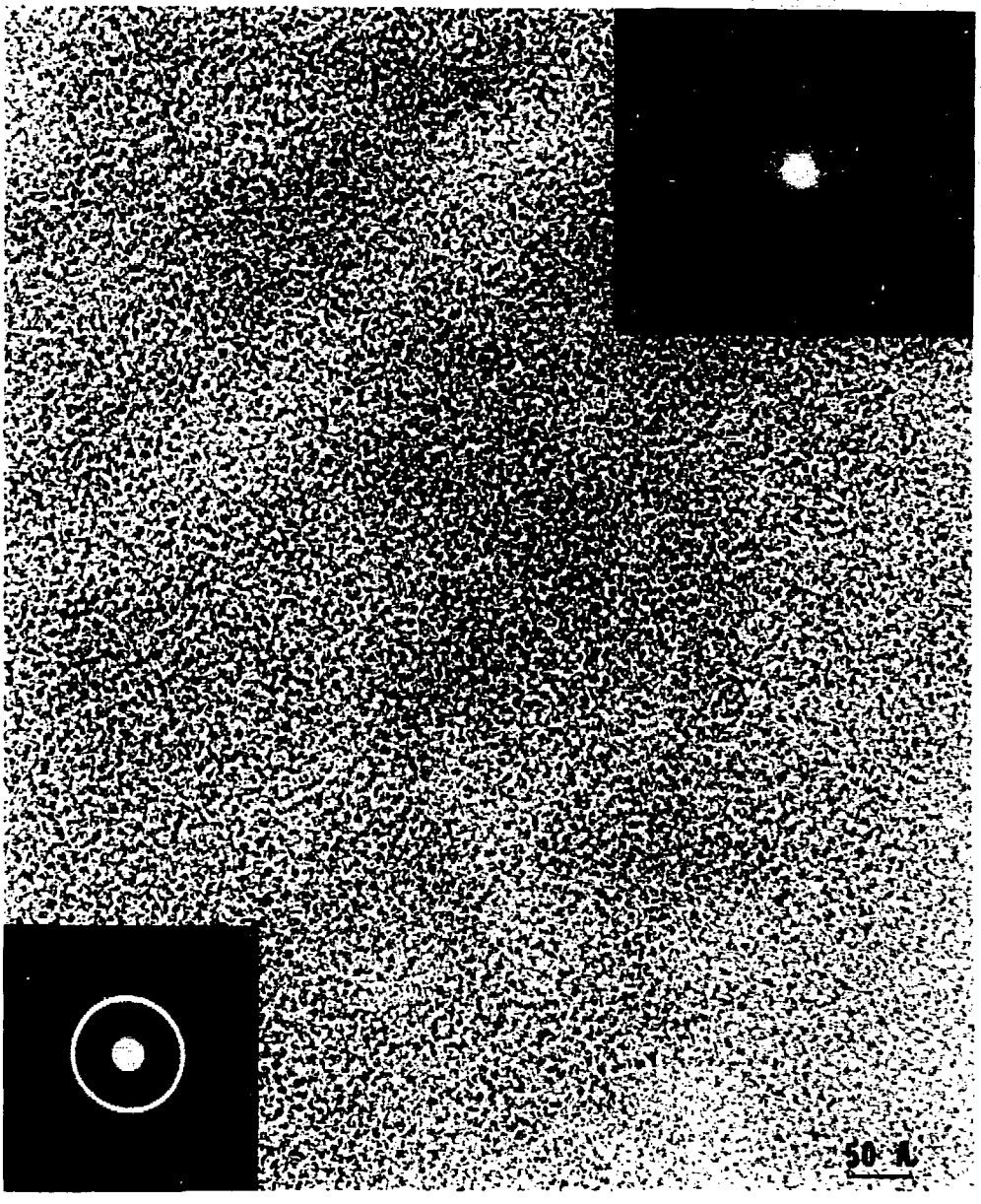

XBB 804 4573

Fig. 8

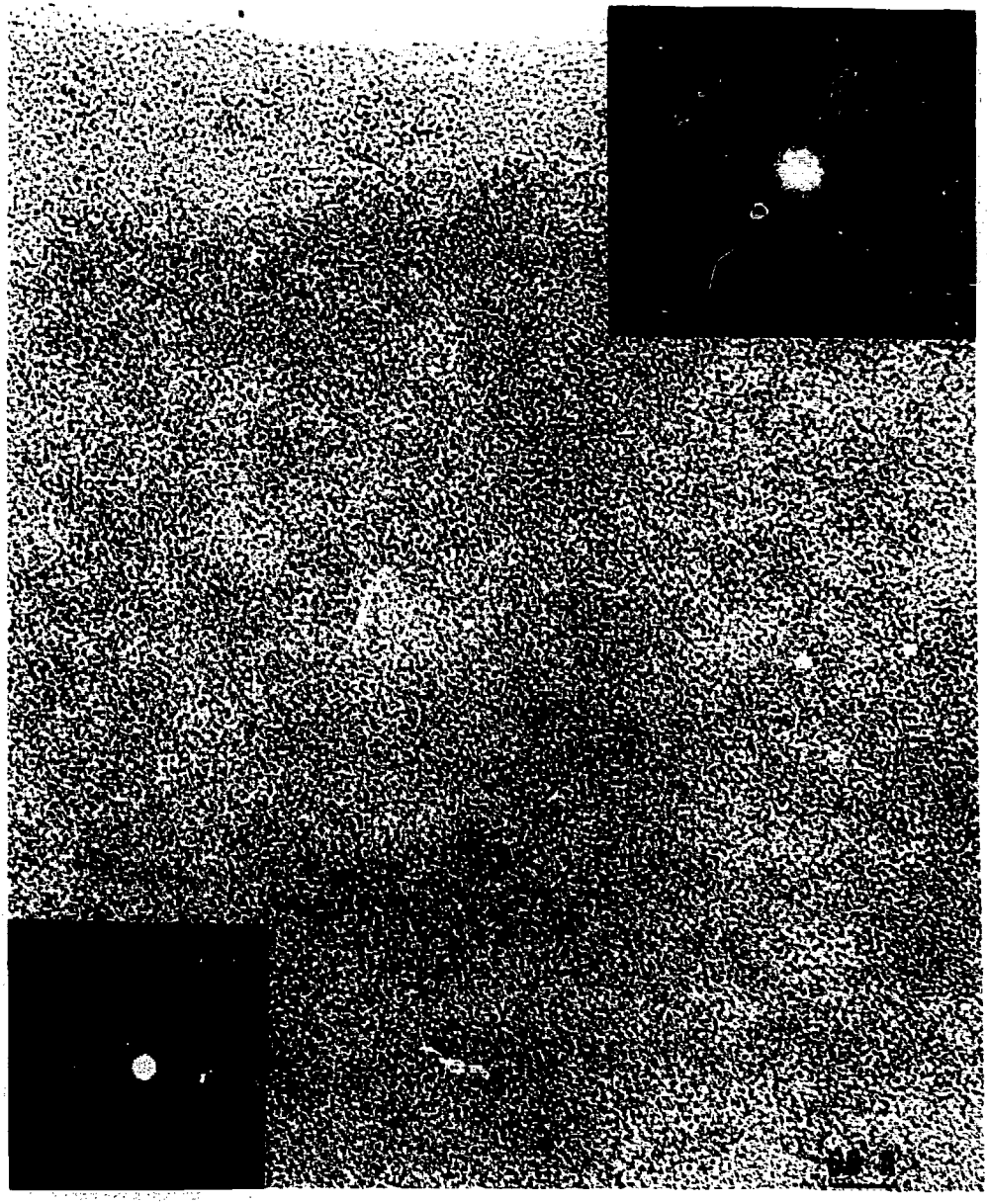

XBB 804 4574

Fig. 9

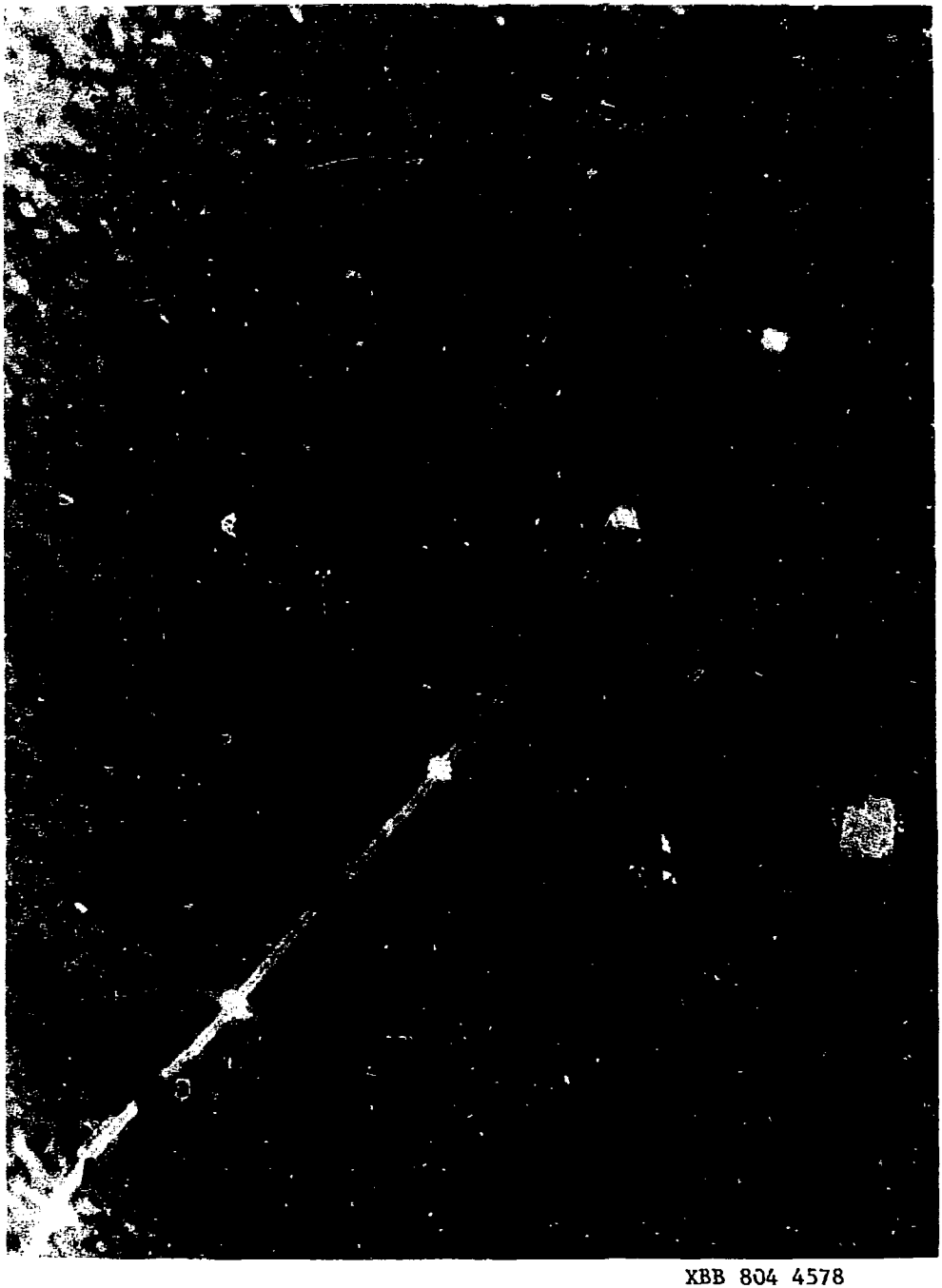

XBB 804 4578

Fig. 10

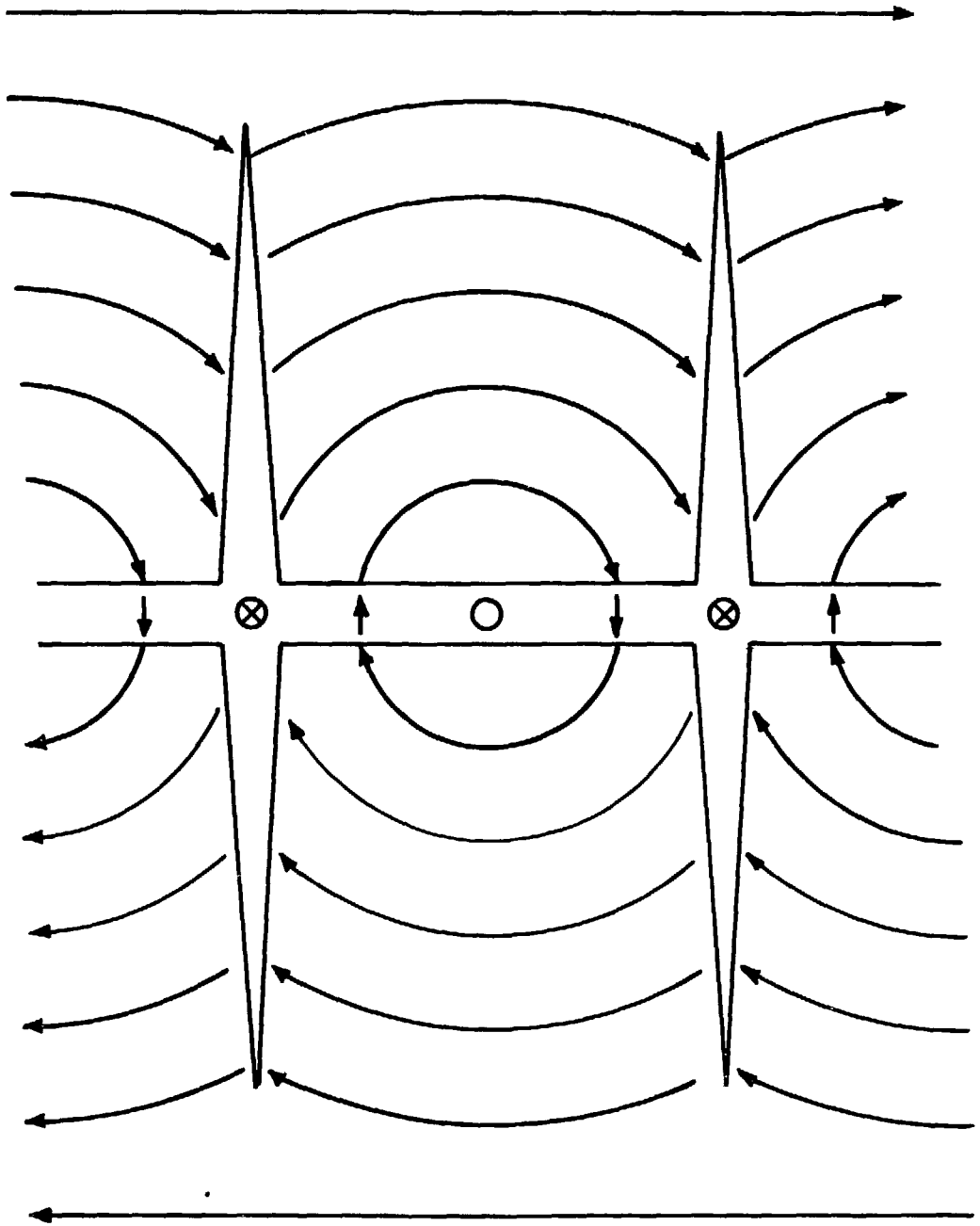

XBL 805-5186

Fig. 11

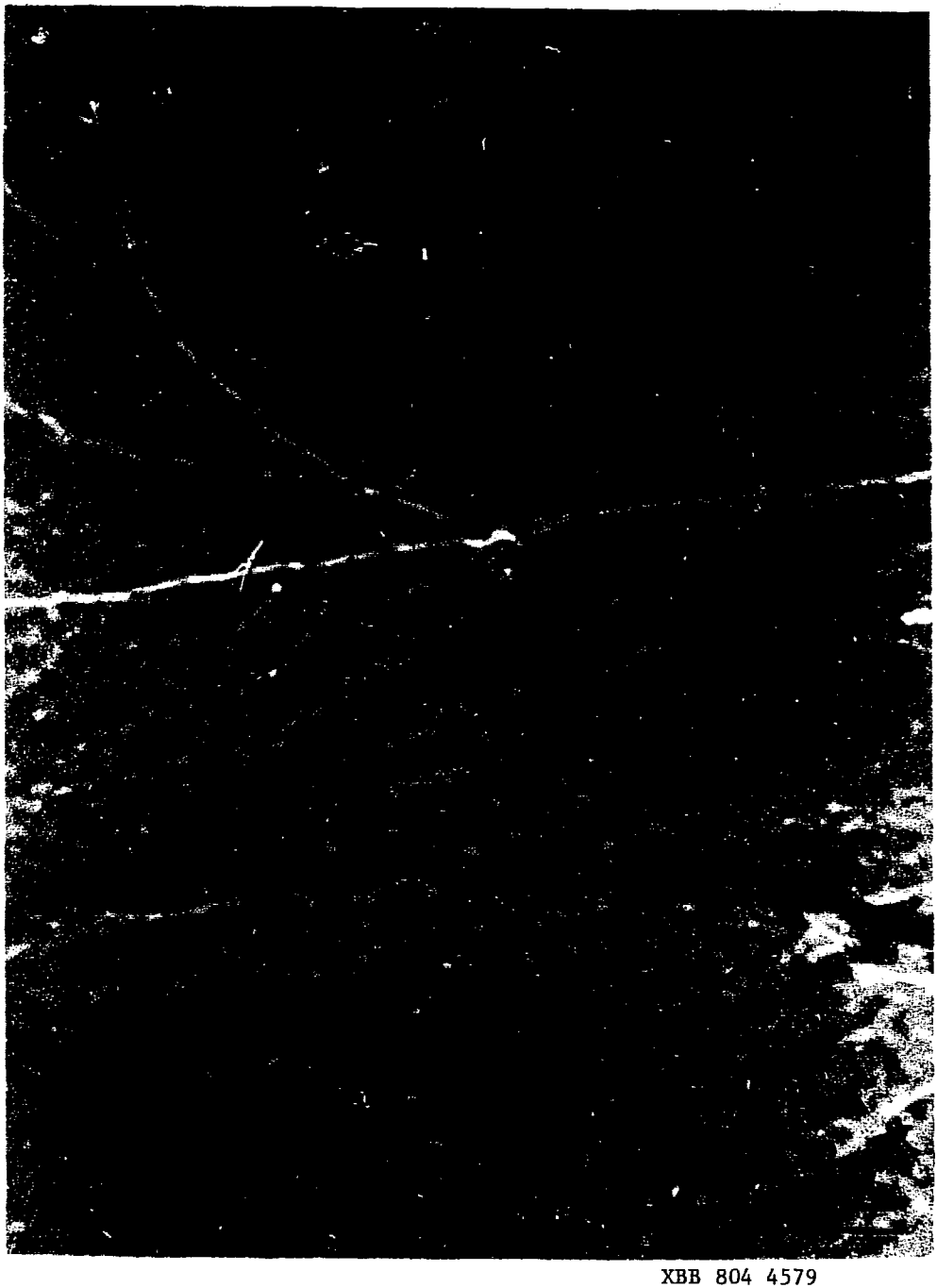

XBB 804 4579

Fig. 12

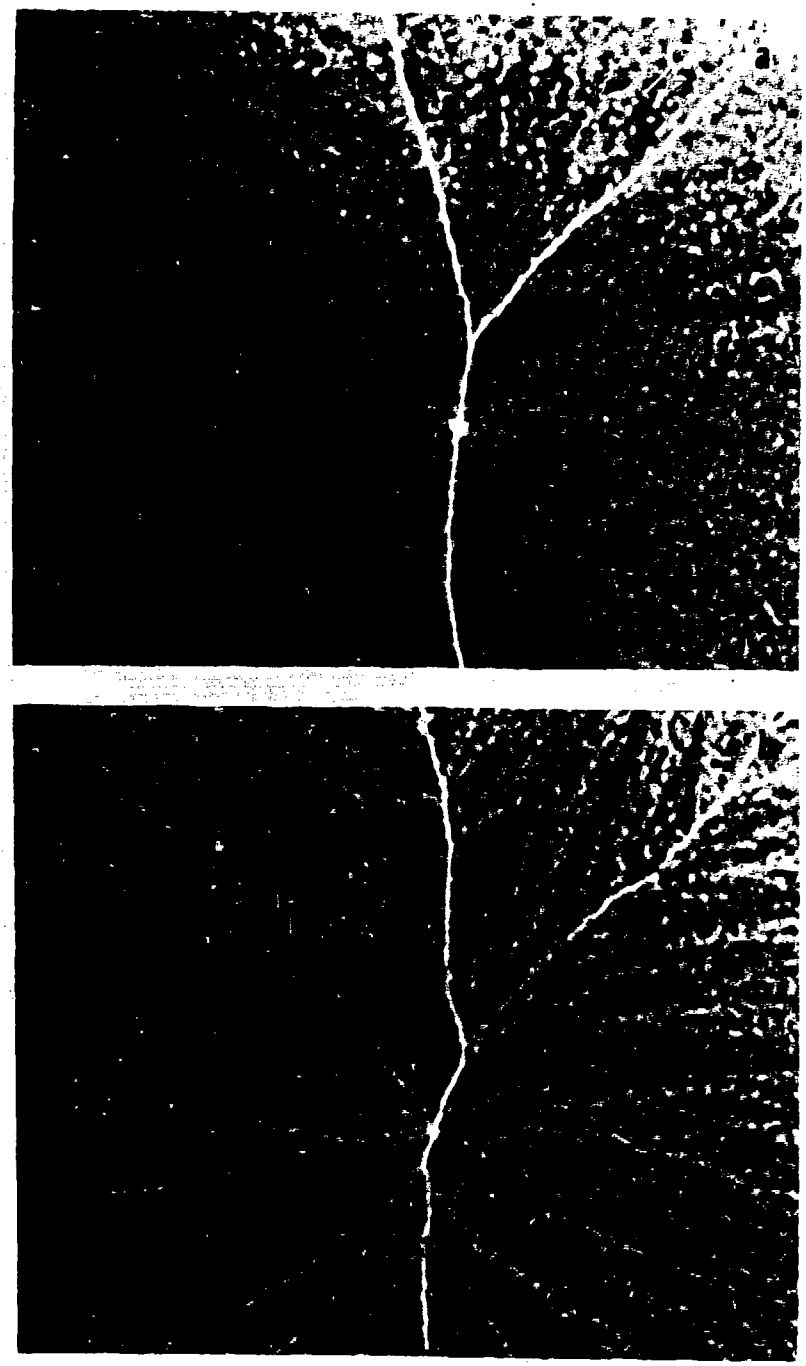

XBB 804 4577

Fig. 13

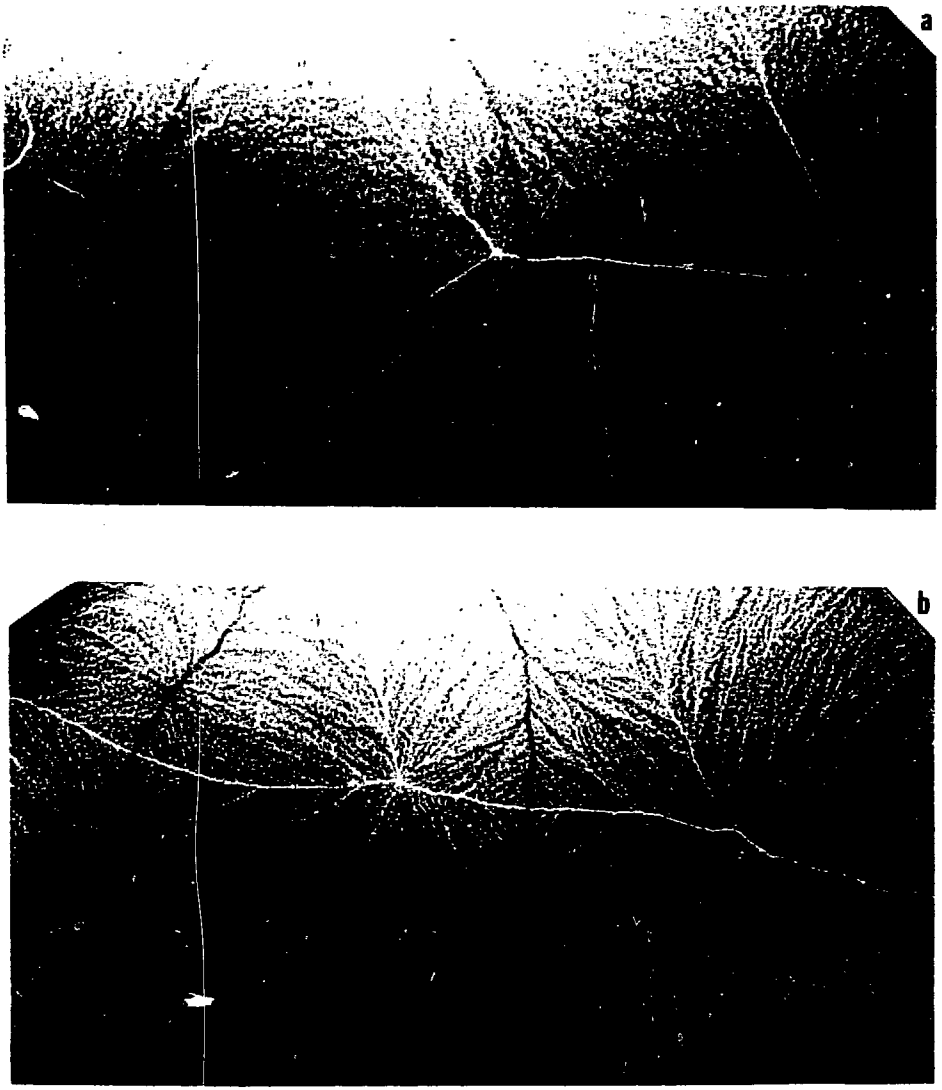

XBB 804 4575

Fig. 14

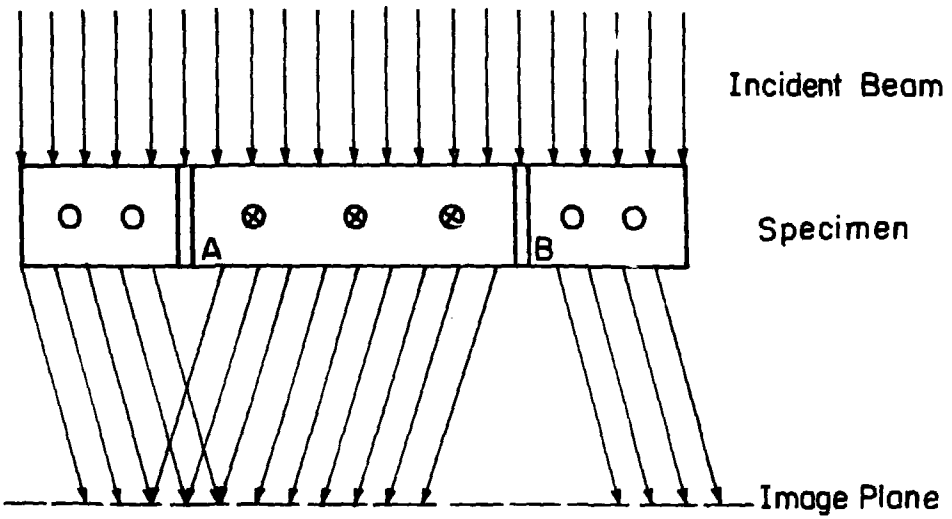

Fig. 15